Received: 7 February 2020 | Revised: 8 April 2020 | Accepted: 8 April 2020

DOI: 10.1002/pat.4939

RESEARCH ARTICLE

polymers for advanced technologies WILEY

Bubbles and collapses: Fire phenomena of flame-retarded flexible polyurethane foams

Martin Günther[1] | Sergei V. Levchik[2] | Bernhard Schartel[1]

[1]Bundesanstalt für Materialforschung und-prüfung (BAM), Berlin, Germany

[2]R&D, ICL-IP America, Tarrytown, New York, USA

Correspondence
Bernhard Schartel, Bundesanstalt für Materialforschung und-prüfung (BAM), Unter den Eichen 87, 12205 Berlin, Germany.
Email: bernhard.schartel@bam.de

Flexible polyurethane foams (FPUF) are easy to ignite and exhibit rapid flame spread. In this paper, the fire phenomena of two standard foam formulations containing tris (1,3-dichloro-2-propyl) phosphate (FR-2) and a halogen-freepoly (ethyl ethylene phosphate) (PNX), respectively, as flame retardants are compared. A multi-methodological approach is proposed which combines standard fire tests as well as new investigatory approaches. The thermophysical properties of the foams were determined by thermogravimetric analysis (TG), reaction to small flames was studied by means of the limiting oxygen index (LOI) and UL 94 HBF test, and the burning behavior was investigated with the cone calorimeter. Further, temperature development in burning cone calorimeter samples was monitored using thermocouples, and rheological measurements were performed on pyrolyzed material, delivering insight into the dripping behavior of the foams. This paper gives comprehensive insight into the fire phenomena of flame-retarded FPUFs that are driven by the two-step decomposition behavior of the foams. LOI and UL 94 HBF tests showed a reduced flammability and reduced tendency to drip for the flame-retarded foams. TG and cone calorimeter measurements revealed that the two-step decomposition behavior causes two stages during combustion, namely structural collapse and pool fire. The flame-retardant mode of action was identified to take place primarily during the foam collapse and be based mainly on flame inhibition. However, some condensed-phase action was been measured, leading to significantly increased melt viscosity and improved dripping behavior for foams containing PNX.

KEYWORDS
burning behavior, flame retardant, flexible PU foam

1 | INTRODUCTION

The profile of properties offered by flexible polyurethane foams (FPUFs) is unique and responsible for their outstanding role in the polyurethane (PU) industry. Today FPUFs are the standard material for cushioning, upholstery, mattresses, etc.[1,2] However, due to their morphology and chemical structure, foams are easy to ignite, exhibit rapid flame spread, and produce a great deal of toxic smoke during combustion.[3,4] Thus, foams are considered to be hazardous materials and their applications necessitate the modification of the material's burning behavior, while the variety of their usage demands different flame-retardant approaches.[5,6] Different studies on the fire phenomena of rigid PU foams (RPUFs) were performed,[7,8] and the burning behavior of flexible foams was studied in greater detail.[9-14] Even

though flexible foams are chemically similar to rigid foams, their burning behavior differs crucially,[9] yet the development of flame retardant strategies requires a comprehensive understanding of the fire phenomena occurring during the combustion of a material.[15] Unlike the morphology of RPUFs, the open cell structure of FPUF allows air flow and makes it prone to the hazard of smoldering combustion.[16,17]

The conventional strategy to modify the burning behavior of foams is to incorporate flame retardants (FRs) into the polymer matrix. There are numerous investigations focused on the synthesis and evaluation of novel FRs.[18-21] A variety of FRs are available for FPUFs, including phosphorus, organophosphorus, nitrogen, halogen, and phosphorus-halogen compounds.[22] But reactive FRs are also used,[23-25] which utilize covalently joined compounds, thus decreasing combustibility of the foam. However, only few additives have commercial relevance.[26]

Halogenated FRs were used successfully for decades, but due to environmental concerns and toxicity, the demand for halogen-free solutions is growing.[27] Investigations that compare established halogenated FRs with halogen-free FRs with a focus on fire phenomena are lacking. The aim of this study is not to evaluate and optimize the performance of different FRs. This paper focuses on the fire phenomena occurring during combustion relating to the structure-property relationships of FPUFs, and compares how they are affected by a halogenated vs a halogen-free FR. For this a set of well-defined samples was prepared, including a reference foam containing no FR, and flame-retarded foams including two different FRs in varied concentrations. The FRs used are Tris(1,3-dichloro-2-propyl) phosphate (TDCP), which is commonly used in the PU industry, and a halogen-free poly(ethyl ethylene phosphate—PNX). A multi-methodological approach is applied to study the fire behavior and fire phenomena in a detailed manner. Forced-flaming condition experiments were performed by means of a cone calorimeter. Thermocouples were inserted into the specimens for cone calorimeter tests to measure the temperature development inside burning specimens. The reaction to small flames and pyrolysis behavior were investigated with the limiting oxygen index (LOI) test, thermogravimetric analysis (TG), and the UL 94 test for horizontal burning of cellular materials (UL 94 HBF). Additionally, cone calorimeter tests in vertical orientation were carried out to study the effect of the FRs on the dripping behavior of the foams. This paper shows likely relations between material properties and resulting burning behavior.

2 | EXPERIMENTAL

2.1 | Materials

Materials were kindly supplied by ICL Industrial Products (Tarrytown, NY). A standard foam formulation and two commercially available FRs were chosen. For the synthesis of the foams, the following precursors were used:

- Polyol - Dow (Midland, MI) Voranol 8136
- Isocyanate - Covestro (Leverkusen, Germany) MONDUR TD 80 Grade A
- Surfactant - Momentive (Waterford, NY) Niax Silicone L-620
- Catalyst 1 - Air Products (Allentown, PA) Dabco 33LV
- Catalyst 2 - Momentive (Waterford, NY) Niax Catalyst A-1
- Catalyst 3 - Air Products (Allentown, PA) Dabco T-10
- Halogenated flame retardant: ICL-IP (Tarrytown, NY) Fyrol FR-2, chlorinated alkyl phosphate FR, Tris(1,3-dichloro-2-propyl) phosphate (TDCP); chemical structure is shown in Scheme 1a
- Halogen-free flame retardant: ICL-IP (Tarrytown, NY) Fyrol PNX, halogen-free polymeric phosphate, Poly(ethyl ethylene phosphate); chemical structure is shown in Scheme 1b

Table 1 lists the formulations of all materials tested in this study. Materials are divided into three groups: *F*-0 is the foam containing no FR; group two contains Fyrol FR-2 in concentrations of 5.0, 7.5, and 10.0 per hundred polyol (php), respectively; the third group uses the same amounts of Fyrol as FR.

2.2 | Sample preparation

The samples were prepared at ICL-IP. The polyols, surfactant, FRs and catalysts were weighed, placed in a mixing beaker and mixed to form a homogeneous solution. Subsequently, the blowing agent (de-ionized water) was added, and after additional mixing, while maintaining its weight against vaporization, the polymeric isocyanate was added. The mixture was stirred at a rate of 5500 rpm at 20°C for approximately 5 seconds and poured into a cardboard cake box. The foam thus formed was held at room temperature for at least 24 hours and then removed from the box and cut into test specimens with the required dimensions using a box cutter.

2.3 | Characterization of density and air flow

Both density and air flow were determined according to ASTM D3574-17. To measure the density, a 1000 mm^3 specimen with no skin or voids was cut from the foams, and then weighed. Air flow was measured with an Air Flow Tester CSI-145 from Custom Scientific Instruments, Inc. (Forks Township, PA, USA) using specimens 50 × 50 × 25 mm^3 in size at standard temperature and a constant pressure differential of 125 Pa across the specimen.

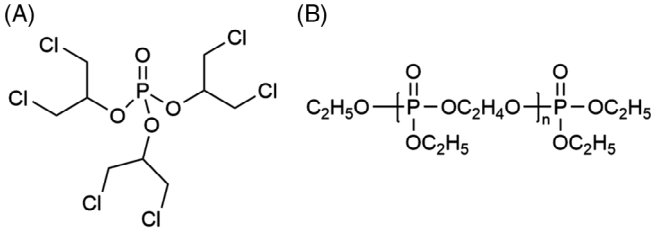

SCHEME 1 Chemical structure of A, TDCP and B, PNX

TABLE 1 Composition of foam materials in php

Additive	*F*	*F*-FR2-A	*F*-FR2-B	*F*-FR2-C	*F*-PNX-A	*F*-PNX-B	*F*-PNX-C
Polyol	100	100	100	100	100	100	100
Isocyanate	47.50	47.50	48.80	50.40	47.50	48.80	50.40
Surfactant	0.8	0.8	0.8	0.8	0.8	0.8	0.8
Catalyst 1	0.19	0.19	0.19	0.19	0.19	0.19	0.19
Catalyst 2	0.06	0.06	0.06	0.06	0.06	0.06	0.06
Catalyst 3	0.32	0.32	0.32	0.32	0.32	0.32	0.32
Water	3.55	3.55	3.70	3.85	3.55	3.70	3.85
FR-2	-	5.0	7.5	10.0	-	-	-
PNX	-	-	-	-	5.0	7.5	10.0

2.4 | Cone calorimeter test

FPUF specimens with dimensions of 100 mm × 100 mm × 50 mm were used. Measurements were performed according to ISO 5660 with a cone calorimeter from Fire Testing Technology (East Grinstead, UK). Several different approaches have been reported for determining a suitable sample thickness of PU foams. Using a higher sample thickness leads to a decreasing heat flux with increasing distance between the cone heater and the sample surface during combustion.[10,28] Yet the cone calorimeter has some limitations when measuring low-density samples, as their weight and fire load are low.[29,30] This can lead to intense scattering of the results.[31] Therefore, a thickness of 50 mm was used for the experiments.

Specimens were stored under standard atmosphere at 23°C and 50% relative humidity for at least 48 hours before the tests. The measurements were carried out using heat fluxes of 20, 25, 35, and 50 kW/m^2 and a separation of 25 mm. In order to protect the sides of the samples and to reduce the unintended effect of edge burning, all samples were wrapped with aluminum foil.

Time to ignition (t_{ig}), heat release rate (HRR), peak heat release rate (PHRR), time to PHRR (t_{PHRR}), total heat released (THR), total mass loss (TML), and effective heat of combustion (EHC) are the parameters that were evaluated. The results reported are the mean values. THR and TML were calculated at flameout, which is defined as the extinguishment of visible yellow flames. All experiments were repeated at least three times, the reproducibility of results was within 10% for all evaluated parameters and is reported as SD.

2.5 | Temperature measurements

To monitor the temperature development inside burning cone calorimeter samples, the specimens were equipped with thermocouples in a vertical orientation. The thermocouples were inserted at depths of 0, 10, 20, and 30 mm from the surface. The tip of the thermocouples was directed toward the cone heater. The thermocouples were placed on the perimeter of a circle with a radius of 20 mm from the center of the specimens and inserted from the bottom up. The falloff of heat flux in this area was reported to have a negligible effect on the results when measuring foams.[9,32] The center area of the specimen experiences a uniform heat flux even at greater distances from the cone heater.[33] The thermocouples used were 0.5 mm sheathed type-*K* omega thermocouples. For each depth, two thermocouples were inserted. Therefore, the temperature for each depth was recorded twice per measurement. Each measurement was carried out in duplicate.

2.6 | Dripping behavior

For the investigation of the dripping behavior, the cone calorimeter setup was changed to vertical orientation to ensure melt flow and to enhance dripping during the test.[34,35] The conical heater of the cone calorimeter was brought into an upright position and a foam specimen with dimensions of 100 × 100 × 50 mm^3 was placed in vertical orientation at a distance of 25 mm. Samples were attached to the sample holder with thin steel wires inserted approximately 3 mm into the foam to avoid interference with dripping, as occurs when steel grids are used to retain the specimen. The external heat flux was adjusted to 50 kW/m^2 to ensure a uniform and distinct foam collapse and melt flow leading to dripping. No ignition source was used during the test to avoid flaming combustion, and thus combustion of the drops were collected in an aluminum catch pan. The dripping pyrolysis products were collected until the entire foam sample had collapsed. The collection was done for two specimens of each material.

After cooling down, the collected material was scraped-off the catch pan and the rheological properties were examined. For this, a cone-plate rheometer (Rheometer MCR 501, Anton Paar, Ostfildern, Germany) was used to exclude the edge effect. The measurements were carried out once in oscillation mode with a deformation amplitude of 5%. A frequency sweep from 100 to 0.1 rad/s was done. The gap was adjusted to 0.8 mm and temperature of the test was 25°C to assure that no further decomposition took place during determination of the rheometric properties.

2.7 | Flammability

The reaction to small flames was measured using the LOI and UL 94 HBF. LOI experiments were carried out according to ISO 4589. Specimens with dimensions of 100 mm × 10 mm × 10 mm were

measured after storage under standard atmosphere at 23°C and 50% relative humidity for at least 48 hours. UL 94 HBF tests were done in accordance with ISO 9772. The tested specimens were 150 mm × 50 mm × 13 mm in size and were stored at 23°C and 50% relative humidity for at least 48 hours. Parameters evaluated are the burning time (t_B), distance burned (L_D), occurrence of burning drops, and burning rate (v).

2.8 | Thermogravimetric analysis

TG was done using a TG 209 F1 Iris (Netzsch Instruments, Selb, Germany). All materials were pyrolyzed under nitrogen atmosphere. A flow of 30 mL/min and a heating rate of 10 K/min were applied. For measuring the mass loss, a sample mass of 5 mg was used. The measurements were carried out using ceramic crucibles. The foams were milled to powder using a CryoMill (Retsch, Haan, Germany) and liquid nitrogen before testing. TG was done at least twice for each material and the mean values are reported. The evaluated parameters are the results of TG as well as differential TG (DTG). $T_{95\%}$ indicates the initiation of pyrolysis and was defined as the temperature of 5 wt.-% mass loss.

2.9 | Visual characterization

The foams' morphology was characterized by visual evaluation of cross sections. The evaluation was done using a Zeiss EVO A10 scanning electron microscope (SEM). Images were taken with an acceleration voltage of 10 kV, and gold sputtering was done to improve image quality by avoiding charging effects.

3 | RESULTS AND DISCUSSION

3.1 | Foam characterization

To render foam materials comparable with respect to their burning behavior, it is necessary to ensure not only that their chemical composition is the same, but also that their morphology does not differ crucially. This is of especially great concern for cellular polymers, since their physical form dominates the material's reaction to applied ignition sources and external heat fluxes.[4,7]

In Figure 1, the SEM micrographs of all materials tested are shown. Each material presents a homogenous cell structure with the typical morphology of FPUF. The cell windows are open, that is, the closed cell content is very low, as is desired for FPUFs.[26]

The density of the tested material ranges from 30.4 to 32.0 kg/m^3 (Table 2), which is typical for FPUF applications such as upholstery and cushioning.[1] The air flow is measured with a flowmeter and gives information on the openness or porosity of the foam.[2] To obtain ideal foam properties, the air flow is desired to be maximized. However, a high air flow is disadvantageous for the flame retardancy of cellular materials. Air flows that are considered typical for FPUF are in the range of approximately 3.0 cfm.[26] Since air flow

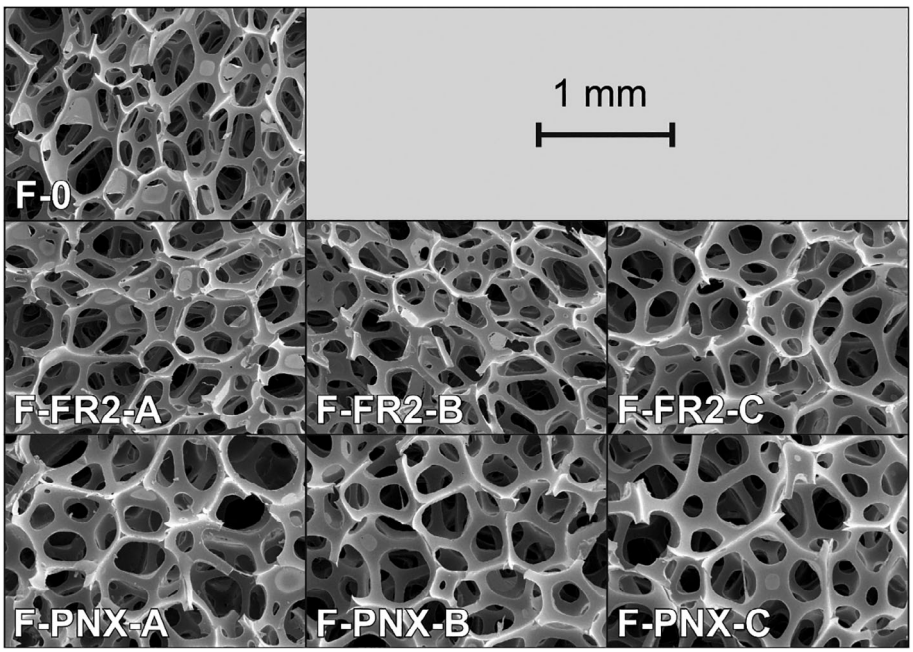

FIGURE 1 SEM micrographs of all materials investigated

TABLE 2 Density and air flow of all materials tested

Property	F-0	F-FR2-A	F-FR2-B	F-FR2-C	F-PNX-A	F-PNX-B	F-PNX-C
Density (kg/m^3)	30.4	30.4	30.4	30.4	32.0	32.0	32.0
Air flow (cfm)	3.3	3.3	3.3	3.3	3.1	3.1	3.1

depends on the opening diameter of well windows as well as the cell size,[36] similar results for air flow measurements of different materials indicate similar cellular structures. For all measured foams, the air flow ranges from 3.1 to 3.3 cfm. Thus, the density and air flow of all materials are reproducible within 10% of their mean value and therefore the materials are deemed to be comparable for this study.

3.2 | Pyrolysis and reaction to small flames

The tested FPUFs exhibit the typical two-step decomposition behavior under nitrogen atmosphere, representing the decomposition to toluene diisocyanate (TDI) and the original polyol.[37,38] This behavior is also known from other PU polymers.[39,40] The TG and DTG graphs are shown in Figure 2 and the results of TG measurements are displayed in Table 3.

The pyrolysis temperature ($T_{95\%}$) decreases with increasing amounts of FR, which is attributed to the overlapping of polymer decomposition and volatilization of the organophosphorus FRs.[41,42] Under nitrogen atmosphere, the amount of residue is negligibly low for *F*-0; after the addition of FRs there was still no significant degree of charring. A maximum of 4.3 wt.-% was measured for *F*-PNX-C. Thus, no relevant effect of a formed protection layer can be expected. However, the slightly increased residue yield for *F*-PNX-C indicates some minor condensed-phase activity of the FRs.[41]

TG and DTG curves reveal that the general decomposition behavior of the foams is hardly changed when the formulation contains FRs. Referring to Table 1, the amount of TDI in the final foam ranges from 31.16 wt.-% for *F*-0 (highest amount) to 30.17 wt.-% for *F*-FR2-C and *F*-PNX-C (lowest amount). This is in good agreement with the mass loss of the first stage of decomposition under TG conditions. This first stage is characterized by the first maximum of the DTG signal, which ranges from 274°C to 289°C. It is reported that in this first step urethane and urea bonds break.[37] Thus, the mass loss of the first stage can be attributed mainly to the volatilization of TDI.[43,44] Some additional mass loss due to volatilization of the FRs may also occur, which explains the higher mass loss at T_{min} for foams containing the halogenated FR-2. In the second step with a maximum temperature of approximately 377°C, most of the polymer's mass decomposes. This second stage of pyrolysis is related to the pyrolysis of the polyol.

The LOI is a measurement for the flame resistance of polymers and describes the minimum amount of oxygen in an oxygen-nitrogen

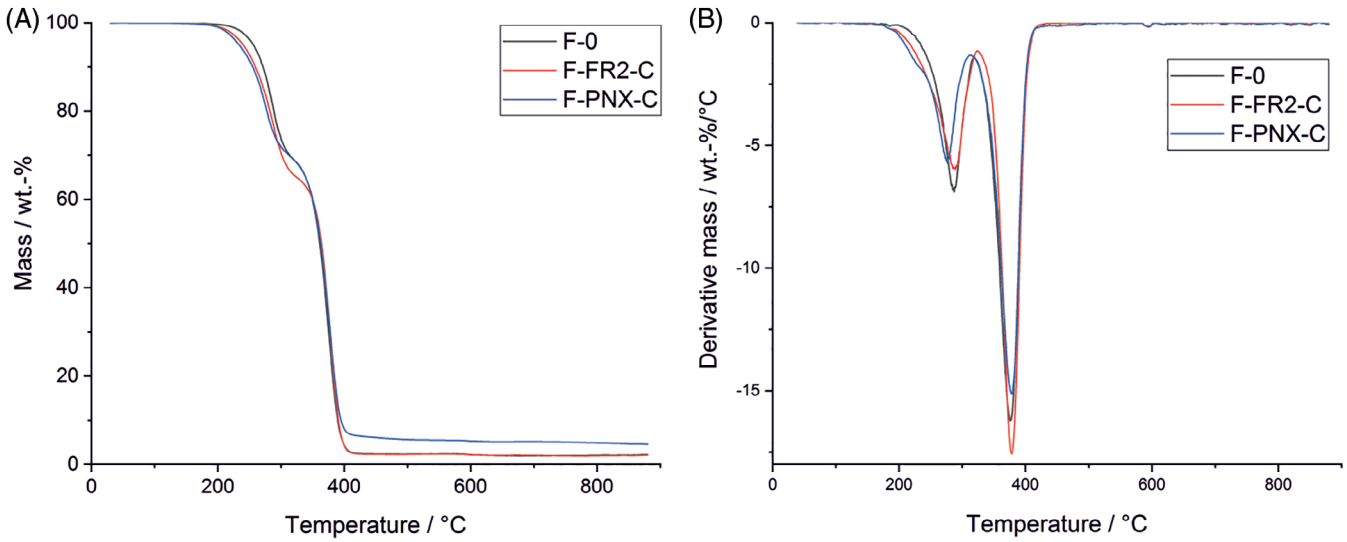

FIGURE 2 A, TG and B, DTG graphs of *F*-0,*F*-FR2-C, and *F*-PNX-C under nitrogen atmosphere [Colour figure can be viewed at wileyonlinelibrary.com]

TABLE 3 TG results under nitrogen atmosphere

Material	$T_{95\%}$ (°C)	T_{max1} (°C)	T_{min} (°C)	Mass loss@ T_{min} (wt.-%)	T_{max2} (°C)	Residue (wt.-%)
F-0	256	287	318	30.7	377	1.8
F-FR2-A	248	288	324	31.7	377	2.7
F-FR2-B	242	289	325	33.7	378	1.9
F-FR2-C	241	288	324	34.9	378	2.3
F-PNX-A	244	277	317	29.2	377	3.0
F-PNX-B	238	277	314	29.6	377	3.9
F-PNX-C	234	274	313	30.1	377	4.3

TABLE 4 LOI results

Material	LOI (vol.-%)
F-0	17.0 ± 0.2
F-FR2-A	20.6 ± 0.2
F-FR2-B	20.7 ± 0.2
F-FR2-C	21.2 ± 0.2
F-PNX-A	21.5 ± 0.2
F-PNX-B	21.8 ± 0.2
F-PNX-C	22.1 ± 0.2

TABLE 5 UL 94 HBF results

Material	t_B (s)	L_D (mm)	Burning drops	ν (mm/min)
F-0	41.0	100.0	yes	146
F-FR2-A	62.4	100.0	yes	96
F-FR2-B	66.0	100.0	no	91
F-FR2-C	68.9	93.0	no	81
F-PNX-A	40.0	60.4	no	91
F-PNX-B	38.1	56.3	no	89
F-PNX-C	33.7	53.6	no	95

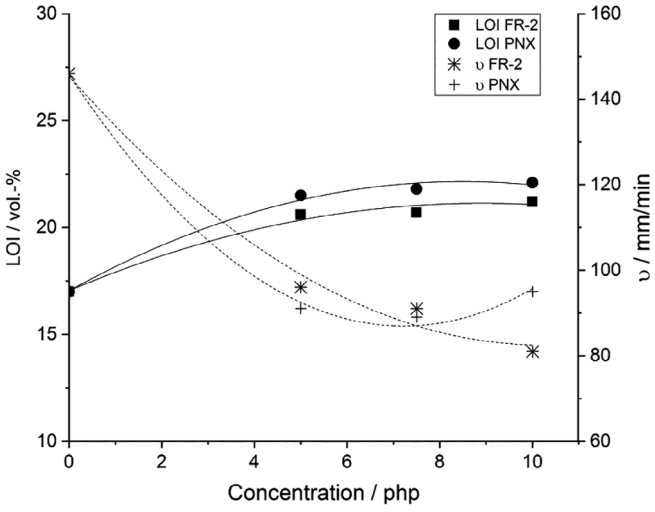

FIGURE 3 Dependency of LOI and ν on the concentration of the FRs

mixture that is necessary to maintain flaming combustion after the ignition of the rod-shaped specimen in a candle-like setup. The measured LOIs are listed in Table 4. It amounts to 17 vol.-% for *F*-0. The foam therefore must be considered as flammable.[45] The addition of FRs significantly increased the LOI up to 22.1 vol.-% for *F*-PNX-C, which is in the range reported for different organophosphorus FRs.[46]

In general, PNX shows superior performance compared to FR-2 in terms of LOI. The dependency of the LOI on the concentration of the FRs is shown in Figure 3. LOI rises at low concentrations and seems to level off when a certain fraction is reached. This behavior in known for phosphorus FRs.[47]

The reaction to small flames was examined by means of the UL 94 HBF test. The foam is placed in a horizontal position and a defined flame is applied. The test is focused on fire phenomena such as self-extinction and dripping. Table 5 lists the test results.

F-0 exhibited no self-extinguishing behavior; the whole specimen burned with a burning rate of 146 mm/min, which is typical for unmodified FPUFs.[48] The addition of FR-2 led to self-extinguishment in the highest concentration and the burning rate was reduced to 91 mm/min. Furthermore, burning drops were eliminated at 5 php of the halogenated FR. The halogen-free FR PNX presented more efficient flame retardancy in the UL 94 HBF test. Burning time and distance burned were significantly decreased, and none of the specimens exhibited burning drops that ignited the underlying cotton. The efficiency increased with increasing additive content.

PNX was determined to be more effective in terms of increasing the LOI and eliminating burning drops. In contrast, FR-2 was better at reducing the burning rate in the UL 94 HBF test. The effects both seem to level off at higher concentrations (Figure 3), and both additives, FR-2 and PNX, are already effective at 5 php. Therefore, they are a promising basis for a multicomponent system in which synergistic effects are utilized to reduce the necessary concentrations of the FRs.[47,49,50]

3.3 | Dripping behavior

Structural collapse and the formation of a pool fire are major characteristics of burning FPUFs and the main hazard of fires involving these materials. In general, melt flow and dripping can be both a benefit and a disadvantage during combustion. They can help by removing heat and mass from the pyrolysis zone, but also contribute to the flame spread by igniting surrounding items (eg, flaming drops or melt flow).[51] For the investigation of dripping behavior, pyrolyzed material was collected as drops in the cone calorimeter experiment using a vertical test setup.

The main parameter influencing the dripping behavior of a polymer in a fire is its melting viscosity as a thermophysical property.[34] Viscosity, which characterizes dripping behavior during combustion, is consistent with the steady-flow viscosity[52]; therefore, dripping occurs at low shear rates.[53] Shear rates ranging from $5 \cdot 10^{-3}$ to $5 \cdot 10^{0}$ were chosen for the measurements. Since FPUF foam is a crosslinked polymer there is no melting as such, but a thermal decomposition resulting in liquid pyrolysis products. The higher their viscosity the lower is the polymer's tendency to drip.[10]

In Figure 4A the complex viscosity is plotted vs the shear rate. The curves of each material are rather horizontal and parallel in the log-log plot. The lowered viscosity of the *F*-0 pyrolysis products can be attributed to two different phenomena. First, a possible explanation is a higher degree of decomposition since shorter chains result in lower viscosity. On the other hand, the formation of char in the melt can also increase viscosity due to enhanced particle-particle interactions.[51,53] At a shear rate of 0.1 s^{-1} the viscosity of *F*-0 pyrolysis

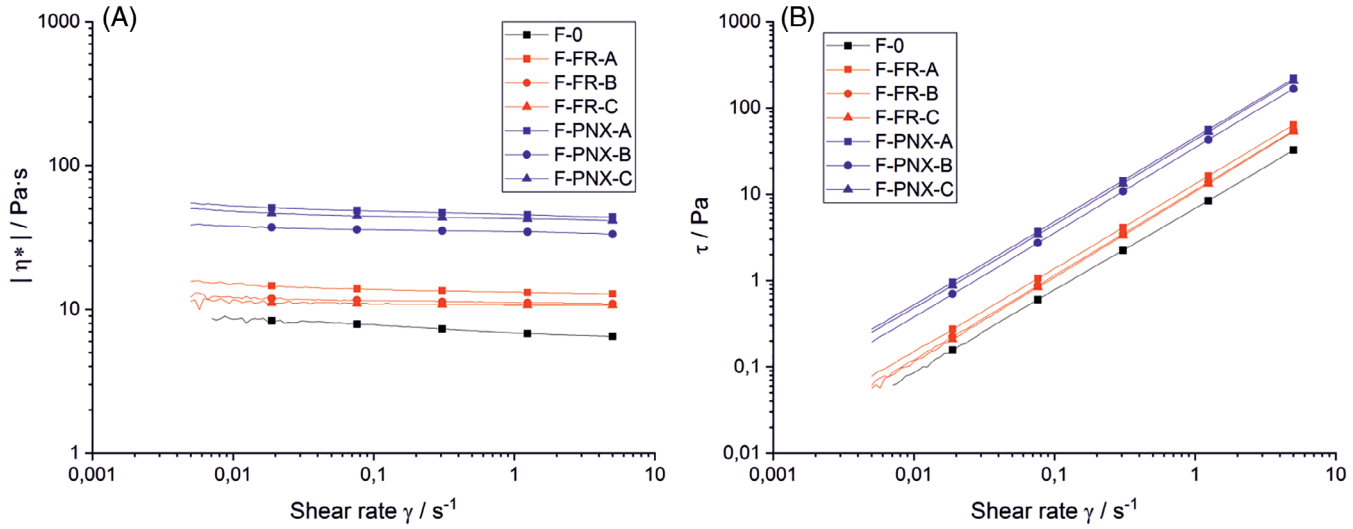

FIGURE 4 Results of rheological measurements of all tested foams: A, complex viscosity and B, shear stress [Colour figure can be viewed at wileyonlinelibrary.com]

products amounts to 7.9 Pa s. It increased to 10.9 Pa s for *F*-FR2-C and to 44.4 Pa s for *F*-PNX-C. The results of complex viscosity correlate well with the residues obtained from TG under pyrolytic conditions (Table 3). The residue was lowest for *F*-0 (1.8 wt-%) and increased to 2.3 wt.-% for *F*-FR2-C and to 4.3 wt.-% for *F*-PNX-C with the addition of 10 php of each FR. Hence, the formation of residue in the melt is considered as a reason for the increased viscosity.

Figure 4B shows shear stress as a function of shear rate. The shear stress of all materials tested decreases linearly with decreasing shear rates, and the lines are parallel to each other. Again, lower shear stress is attributed to lower viscosity, caused by increased char formation as shown in TG experiments. This indicates a reduced tendency to drip and decreased melt flow for the foams containing FRs. The results of rheological measurements are in accordance with the results from the UL 94 HBF test and show that the tendency to drip is reduced for the flame-retarded foams compared to *F*-0. Foams containing PNX as FR exhibit no dripping in the UL 94 HBF test since the complex viscosity of the measured drops is significantly increased.

3.4 | Fire behavior

All foams exhibited the typical burning behavior (Figure 5) that is known from FPUFs and shown in Figure 6.[9] Once the foams were exposed to the external heat flux, the material ignited within seconds. The reason for this is their low thermal inertia, which is caused by the low thermal conductivity of the material. A single cell strut behaves like a thermally thin material and reaches the temperature of ignition much faster than a bulk material, since the heat conduction into the material is limited.[4,54]

After ignition, a thin and liquid layer of intermediate pyrolysis products is formed. This layer moves from the top of the specimen all the way down to the bottom as the foam sample collapses and a subsequent pool fire occurs. This collapse often is referred to as "melting." Yet, PU is a crosslinked polymer, meaning that the term "melting" is misleading. The collapse is due to the thermal decomposition of the material generating liquid pyrolysis products.[12] The result is the formation of a viscous liquid layer consisting of the pyrolyzed foam.

Table 6 shows the cone calorimeter results that were obtained using an external heat flux of 20 kW/m^2. The t_{ig} ranges from 8 to 10 seconds and does not significantly differ when FRs are included into the formulation of the foams, since their early ignition behavior is dominated by the physical form of the cellular polymers.[4] The PHRR is the maximum of the HRR as a function of time and is often considered to be the most important fire hazard.[33] PHRR amounts to 375 kW/m^2 for *F*-0, and is slightly increased for the FR-2 foams and significantly increased for foams containing PNX. A possible explanation for this effect is the two-stage combustion of the foams. In the first stage, when the foam collapses and the FR is vaporized, making it available for flame inhibition and some minor condensed-phase action, more pyrolysis products are left in the melt pool compared to *F*-0. These additional products of reactions taking place in the condensed phase then burn simultaneously with the polyol in the pool fire stage. Since the pool fire behaves like a thermally thin material, that is, all of its mass burns simultaneously, its PHRR strongly depends on the fire load.[33] It was reported that residual TDI has also been found in the pool fire, contributing to combustion.[55] This effect is slightly more pronounced for foams containing PNX, since the FR seems to be more effective according to LOI and UL 94 HBF results and flame inhibition takes place only in the first stage of combustion.

The increase in PHRR and their slightly earlier occurrence also leads to a slight increase in the fire growth rate (FIGRA), which equals the maximum quotient of HRR(t)/t. The PHRR/t_{ig} probably represents a better approach to quantify the flame spread that is not directly measured in the cone calorimeter. However, since t_{ig} is typically quite

TABLE 6 Cone calorimeter results, heat flux: 20 kW/m^2

	t_{ig} (s)	PHRR (kW/m^2)	FIGRA (kW/m^{2}s)	THR (MJ/m^2)	Residue (wt.-%)	EHC (kJ/g)	TSR (m^2/m^2)	CO yield (g/kg)
F-0	10 ± 2	375 ± 17	9.0 ± 0.6	39 ± 1	0.0 ± 0.1	26.0 ± 0.1	286 ± 66	18 ± 1
F-FR2-A	8 ± 1	417 ± 6	7.7 ± 0.3	37 ± 1	0.0 ± 0.1	24.1 ± 0.2	418 ± 28	37 ± 1
F-FR2-B	9 ± 1	432 ± 16	7.4 ± 0.1	36 ± 2	0.0 ± 0.1	23.5 ± 0.1	486 ± 24	46 ± 1
F-FR2-C	9 ± 1	425 ± 24	7.0 ± 0.5	34 ± 1	0.0 ± 0.1	22.5 ± 0.2	519 ± 45	54 ± 1
F-PNX-A	10 ± 1	451 ± 10	7.8 ± 0.3	36 ± 1	0.0 ± 0.1	23.9 ± 0.3	525 ± 47	48 ± 1
F-PNX-B	10 ± 1	443 ± 26	7.3 ± 0.4	34 ± 1	0.0 ± 0.1	23.3 ± 0.2	526 ± 36	58 ± 1
F-PNX-C	10 ± 1	465 ± 20	7.4 ± 0.3	34 ± 1	0.0 ± 0.1	22.7 ± 0.5	608 ± 22	65 ± 1

low for foams, small variations lead to large effects on the quotient, with the result that it becomes insignificant. For most polymers the FIGRA can be expressed as the quotient of PHRR/t_{PHRR}. However, as there are exceptions, it is extremely important to pay attention to the beginning of the HRR curve.[56] For FPUFs exhibiting a rapid flame spread after ignition, the FIGRA must be taken at the slope of the first stage of combustion; otherwise FIGRA will be underestimated. The FIGRA of *F*-0 amounts to 9.0 kW/m^{2}s and decreased to 7.0 kW/m^{2}s for *F*-FR2-C and 7.4 kW/m^{2}s for *F*-PNX-C, indicating a reduced flame spread of the flame-retarded foams.

Observations during cone calorimeter tests indicated some char formation on the surface in the form of black dots on top of the pyrolysis zone. Yet this char did not cover the whole surface, since the amount was insufficient and the surface was in constant movement due to the low viscosity and intense bubbling of the pyrolysis zone. This effect was observed for all flame-retarded foams in this study. All tested materials burned in the cone calorimeter without residue. Thus, no effect of a protective layer is present as is known for rigid PU foams.[8]

The integral of HRR over time is referred to as THR and represents a measurement for the fire load of a material. The THR decreased from 39 MJ/m^2 for the non-flame retarded foam to 34 MJ/m^2 for the foams containing the highest amount of FR. A reduced fire load indicates incomplete combustion, which can be caused either by charring or by lowered combustion efficiency. Since none of the foams yielded a significant amount of residue and thus no protective layer was formed, the reduction of THR is related mainly to a decreased EHC.

The EHC of a material was expressed as the total heat evolved per TML of the cone calorimeter test. For low-weight samples this gives more reliable results. The EHC of *F*-0 amounts to 26 kJ/g and is significantly reduced to 22.5 kJ/g for F-FR2-C and 22.7 kJ/g for *F*-PNX-C, respectively. This indicates incomplete combustion and therefore gas-phase activity of the FRs.[33,57] Smoke production and CO yield are both major fire hazards and typically increase when FRs active in the gas phase lead to incomplete combustion.[33] Hence, TSR and CO yield are significantly increased when the foam contains FRs, and the effect becomes more pronounced when the concentration of the additives rises. This effect is known for organophosphorus FRs and indicates incomplete combustion under forced flaming conditions.[58] The increase of CO yield is significantly greater for PNX than for foams containing FR-2. For polymers without FRs, the EHC is the product of the EHC of the volatiles (h_c^0) and the combustion efficiency (χ). The EHC of foams containing a FR was reduced by the factor of χ. This factor describes how effectively a fuel is combusted in the flame and ranges between 0 and 1. Due to the well-ventilated cone calorimeter setup, χ is typically close to 1. Yet, flame inhibition leads to incomplete combustion and decreases χ. The chemical structure of the FPUFs investigated in this paper is considered to be the same since their formulations differ only by the FR added as a filler. Thus, h_c^0 is assumed to be the same for *F*-0 and the flame-retarded foams, implying that the change in EHC is caused solely by a decreased χ.[8] Therefore, flame inhibition is identified as a major flame retardant mode of action for foams containing FR-2 and PNX. This is in good agreement with the literature. The flame retardant mode of action of FR-2 is reported to be based on some condensed-phase action and flame inhibition in the gas phase.[41,59,60] Due to results of TG and cone calorimeter experiments, the same mode of action seems to be relevant for PNX. However, since PNX is a polymeric FR with a molecular weight of approx. 900 Da, it decomposes prior to evaporation as it is known for various phosphorus FRs.[42,61]

Table 7 displays the cone calorimeter test results obtained with a heat flux of 50 kW/m^2. The measured t_{ig} decreased to 2 to 3 seconds for all materials due to the higher external heat flux.[62] Further, the PHRR increased with heat flux and occurred earlier, leading to a drastically increased FIGRA.[33] Compared to the results obtained at 20 kW/m^2 heat flux, the THR decreases equally with the use of the FRs. A dependency of some of the measured parameters on the concentration of the FRs was found. THR and EHC clearly decrease with increasing FR content due to flame inhibition and the resulting incomplete combustion of the foam. The lowered χ causes a crucial increase in TSR and CO release. For the PHRR and FIGRA no direct correlation with the FR concentration was measured, but PHRR generally increased and FIGRA decreased compared to *F*-0. The increase was more pronounced for the foams containing PNX. Results for heat fluxes of 25 and 35 kW/m^2 are reported in the Supporting Information (Tables S1 and S2).

A separate series of cone calorimeter tests was performed in which the specimens were equipped with thermocouples. During the test, the temperature development inside burning cone calorimeter specimens was measured on the surface and at depths of 10, 20, and

TABLE 7 Cone calorimeter results, heat flux: 50 kW/m^2

	t_{ig} (s)	PHRR (kW/m^2)	FIGRA (kW/m^{2}s)	THR (MJ/m^2)	Residue (wt.-%)	EHC (kJ/g)	TSR (m^2/m^2)	CO yield (g/kg)
F-0	2 ± 1	901 ± 97	24.5 ± 2.9	41 ± 1	0.0 ± 0.1	26.1 ± 0.7	263 ± 12	25 ± 1
F-FR2-A	3 ± 2	854 ± 71	18.2 ± 2.5	38 ± 1	0.2 ± 0.1	23.8 ± 0.1	463 ± 23	46 ± 3
F-FR2-B	2 ± 1	928 ± 29	19.5 ± 0.5	37 ± 2	0.0 ± 0.1	23.4 ± 0.3	519 ± 12	53 ± 5
F-FR2-C	3 ± 1	881 ± 88	16.5 ± 1.7	34 ± 1	0.0 ± 0.1	22.4 ± 0.2	534 ± 22	61 ± 3
F-PNX-A	3 ± 1	1070 ± 26	19.4 ± 1.2	38 ± 1	0.1 ± 0.1	23.8 ± 0.1	519 ± 18	55 ± 3
F-PNX-B	2 ± 1	1037 ± 59	19.9 ± 2.0	35 ± 1	0.0 ± 0.1	23.0 ± 0.4	545 ± 12	69 ± 5
F-PNX-C	2 ± 1	1023 ± 58	20.8 ± 1.4	34 ± 1	0.9 ± 0.1	22.9 ± 0.3	583 ± 47	78 ± 4

30 mm. HRR was monitored simultaneously and the results are shown in Figure 5 for A, *F*-0; B, *F*-FR2-C; and C, *F*-PNX-C.

Before the pyrolysis front approaches the thermocouples, measured temperatures remain nearly at ambient temperature, indicating that the thermal conduction into the foam is rather limited. This is in good agreement with experiments performed on rigid PU foams.[7] The steep rise of temperature to approx. 800°C indicates the pyrolysis front moving through the sample and therefore the collapse of the material's cellular structure. After the foam collapses, the measured temperatures equal the temperatures of the flame. Since the foam collapses quickly, it is hard to determine the actual temperature of the pyrolysis zone.[9] However, Figure 5D shows a kink in the temperature

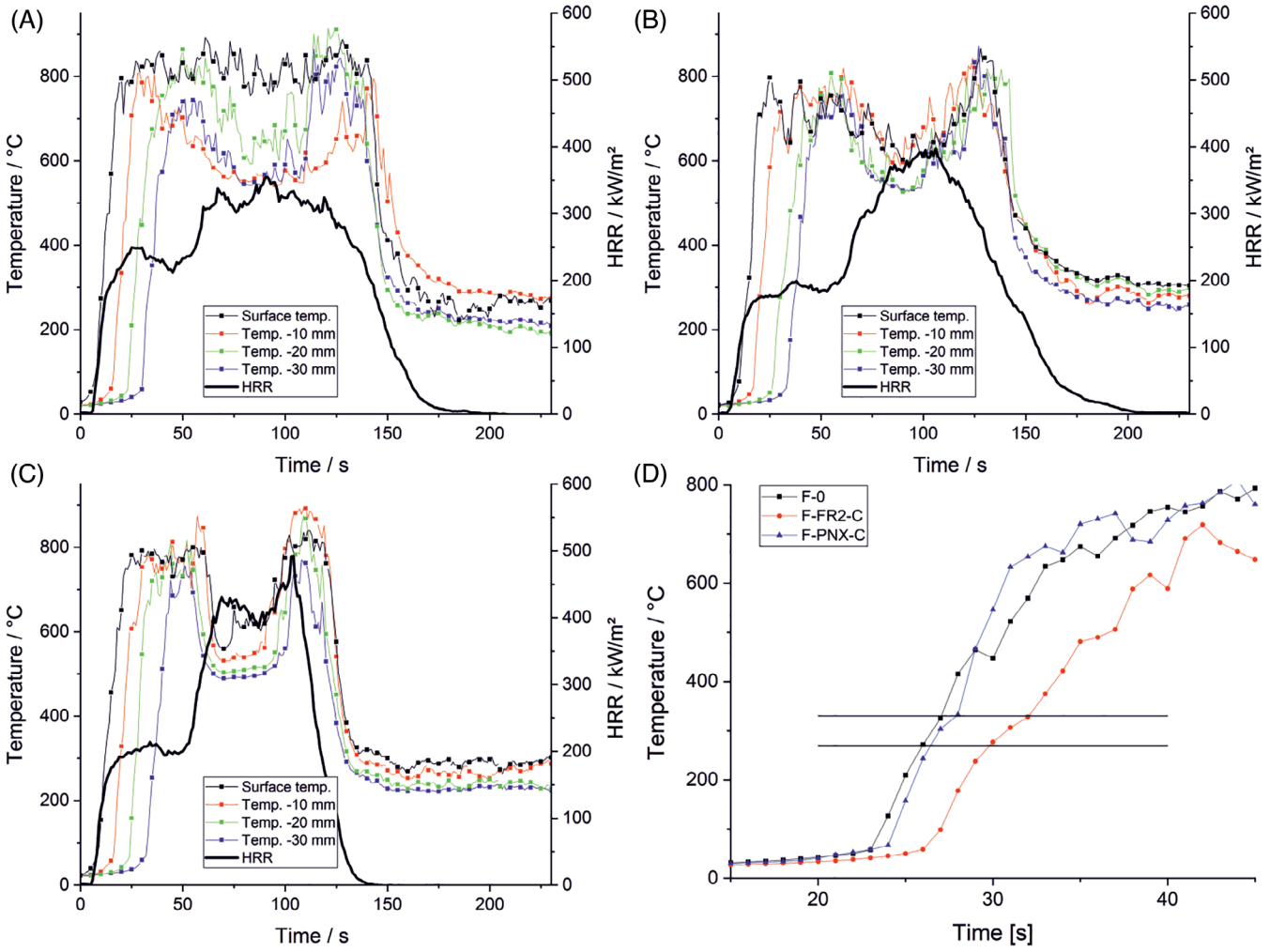

FIGURE 5 Temperature development inside burning cone calorimeter specimens and HRR of A, *F*-0; B, *F*-FR2-C; and C, *F*-PNX-C and D, temperature at depth of 20 mm; heat flux: 25 kW/m^2 [Colour figure can be viewed at wileyonlinelibrary.com]

curve approx. Between 270°C and 330°C, measured at a depth of 20 mm from the surface. Its onset correlates with the T_{max1} and its offset with the transition from first to second decomposition step (T_{min}). Hence, the temperature range indicates that the temperatures of the pyrolysis zone are roughly between 270°C and 330°C, correlating with the decomposition temperature of the first step from TG.

The measured temperatures dropped when the structural collapse of the foams was complete and the transition to the pool fire stage took place. This effect seems to be even more pronounced with the addition of FR, as shown in Figure 5B,C. A possible explanation for this may be that even though the rate of heat release had already risen to its maximum, measured temperatures are lower since the measurements take place in the colder area of the flame plume, which is much higher than the aluminum tray containing the thermocouples and the burning pool of pyrolysis products. As the flame plume gets smaller, thermocouples reach the area of higher flame temperatures. This is followed by flameout. After flameout the measured temperatures represent the radiation of the cone heater.

Based on the history of the HRR curve, as shown in Figure 6 for *F*-0, the foam's combustion can be divided into two stages, namely structural collapse and the stage of pool fire. It is salient that there is also a kink in the history of THR, and that the slope of mass loss decreases in the same region where the junction from foam collapse to pool fire takes place. In the first step of foam combustion, the urethane and urea bonds are reported to break, which leads to the formation of TDI and the polyol.[37] Therefore, the heat release in the first step is due mainly to the combustion of the TDI. The polyol is left as a melt pool and burns in the second stage as a single burning layer, which is then responsible for the majority of heat release.[9] What remains is the question of whether the two-step burning behavior is caused by the decomposition behavior that was observed in TG experiments.

To address this question, the first and second stages were separated by visual evaluation of the HRR curves. The point of sudden slope increase was determined as the junction to the pool fire stage. This correlated temporally with the observations made during the cone calorimeter test, where the initial collapse was followed by a rapidly growing flame plume when the pool fire took place. Table 8 compares the TML, THR, EHC, and average HRR (avHRR) of all tested materials in the first and second stages of combustion. The avHRR of the pool fire stage is not evaluated, since different flameout times affect this parameter such that it loses its significance.

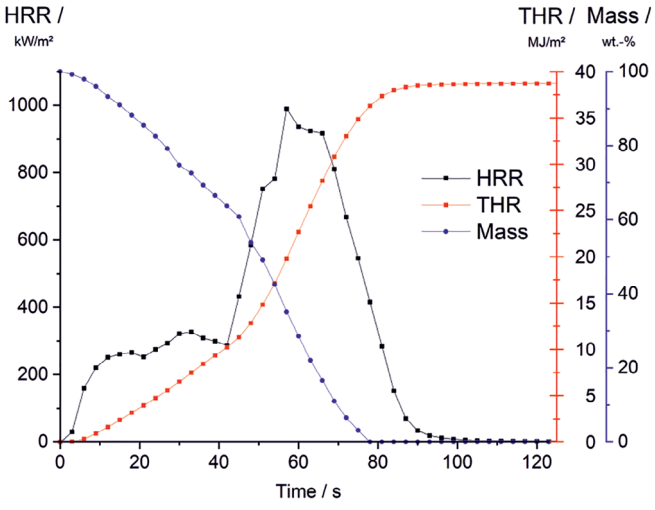

FIGURE 6 HRR, THR, and mass loss of *F*-0 at a heat flux of 50 kW/m^2 [Colour figure can be viewed at wileyonlinelibrary.com]

The results show that TML_1 amounts to 35 wt.-% for F-0 and increases to 39 wt.-% for *F*-FR2-C and *F*-PNX-C. This increase can be attributed to the vaporization of the FR. Further, the mass loss of the first stage as measured in the cone calorimeter correlates well with the mass loss of the first decomposition step that was determined in TG. Under pyrolytic conditions the mass loss ranged from 30 to 35 wt.-%. The difference is connected to the differences in the experimental setup: while TG measures under pyrolytic conditions, the cone calorimeter simulates a fire scenario. Thus, the increased mass loss in the cone calorimeter can be attributed to some overlap between TDI and polyol decomposition. While the foam collapse is still taking place, some of the polyol already decomposes, contributing to the mass loss of the collapse stage.

Furthermore, the measurements show that the reduction in the EHC due to FRs is significant only in the first stage. This is due to the release of the flame retardant into the gas phase, where it is exploited for flame inhibition. When pool fire takes place, most of the FR is already vaporized. EHC_2 therefore is hardly affected by FRs with respect to *F*-0. In contrast, EHC_1 for the foams containing FR-2 or PNX decreases significantly.

THR_1 and THR_2 are significantly decreased in both stages for F-FR2-C and F-PNX-C compared to *F*-0. The reduction in THR_1 is connected to the decreased EHC_1 for the flame-retarded foams, leading to a reduction in heat release despite the increased TML_1. In contrast, the decline in THR_2 is caused by the decreased TML_2, since EHC_2 remains nearly unchanged by the incorporation of FRs.

Since a crucial difference in the EHC of the first and the second stages of foam combustion was measured for *F*-0 as well, it can be derived that the two-stage decomposition behavior that was determined under TG conditions accounts for the two steps of combustion in the cone calorimeter experiment. The differences in EHC also cause the substantial incline in HRR during the pool fire stage. This effect is further enhanced since the melt pool burning in the second stage behaves like a thermally thin material, with, the whole sample burning at once so that the apparent PHRR becomes dependent on the fire load of the liquid pool.[33]

The $avHRR_1$ shows the effect of the FRs in the first stage of combustion. Compared to *F*-0, the average rate of heat release is significantly decreased. Again, this gives evidence of the FRs being active only in the first stage but not improving burning behavior during the pool fire. Even though the use of FRs hardly affects overall burning characteristics, the reduction of the first peak helps passing flammability tests.[63] For heat fluxes of 20, 25, and 35 kW/m^2, the corresponding values are listed in the Supporting Information (Table S3, S4, and S5).

TABLE 8 THR, EHC, of first and second stage of combustion and $avHRR_1$, heat flux: 50 kW/m^2

	TML_1 (wt.-%)	TML_2 (wt.-%)	THR_1(MJ/m^2)	THR_2(MJ/m^2)	EHC_1 (kJ/g)	EHC_2 (kJ/g)	$avHRR_1$ (kW/m^2)
F-0	35 ± 2	65 ± 4	11 ± 1	29 ± 1	19.7 ± 0.9	29.9 ± 1.9	255 ± 9
F-FR2-A	36 ± 1	64 ± 1	9 ± 1	29 ± 1	16.1 ± 0.2	28.1 ± 0.3	203 ± 12
F-FR2-B	37 ± 1	63 ± 1	9 ± 1	29 ± 1	14.9 ± 0.2	28.2 ± 0.6	207 ± 7
F-FR2-C	39 ± 3	61 ± 2	8 ± 1	26 ± 1	13.8 ± 0.5	28.1 ± 1.0	179 ± 16
F-PNX-A	36 ± 3	64 ± 3	9 ± 1	29 ± 1	16.2 ± 0.3	28.0 ± 0.8	202 ± 16
F-PNX-B	36 ± 3	64 ± 2	8 ± 1	27 ± 1	15.5 ± 0.8	27.2 ± 0.7	205 ± 14
F-PNX-C	39 ± 2	61 ± 2	9 ± 1	25 ± 1	15.5 ± 0.4	27.5 ± 0.7	216 ± 12

In Figure 7, the effect of different heat fluxes on the HRR is presented for *F*-0 and each FR foam containing the highest amount of FR. Each curve exhibits the characteristics of a two-step burning behavior. In the first stage, ignition is followed by a sharp rise in HRR and a plateau-like phase of burning which represents the structural collapse. Subsequently, the pool fire takes place, which is characterized by a sharp rise in the HRR and the PHRR. After this, HRR drops until flameout occurs. The two stages become more obvious when the external heat flux rises, and HRR generally rises with increased heat flux.[33] Figure 7D shows the PHRR and $avHRR_1$ plotted versus heat flux. In this plot, the detrimental effect of the FRs on the PHRR as well as the improvement in $avHRR_1$ becomes obvious. Both

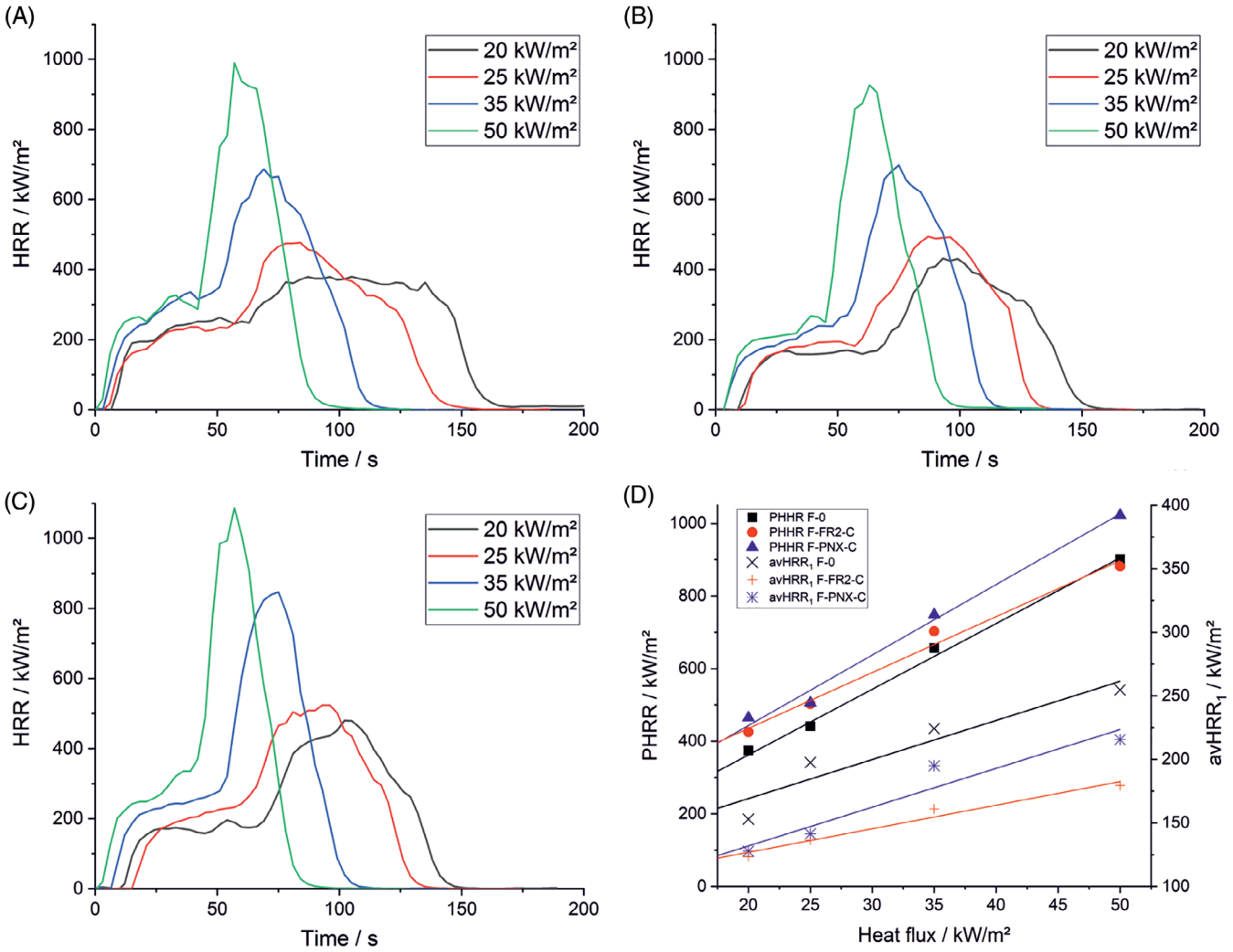

FIGURE 7 HRR curves for A, *F*-0, B, *F*-FR2-C, and C, *F*-PNX-C and D, PHRR and avHRR1 plotted vs heat flux [Colour figure can be viewed at wileyonlinelibrary.com]

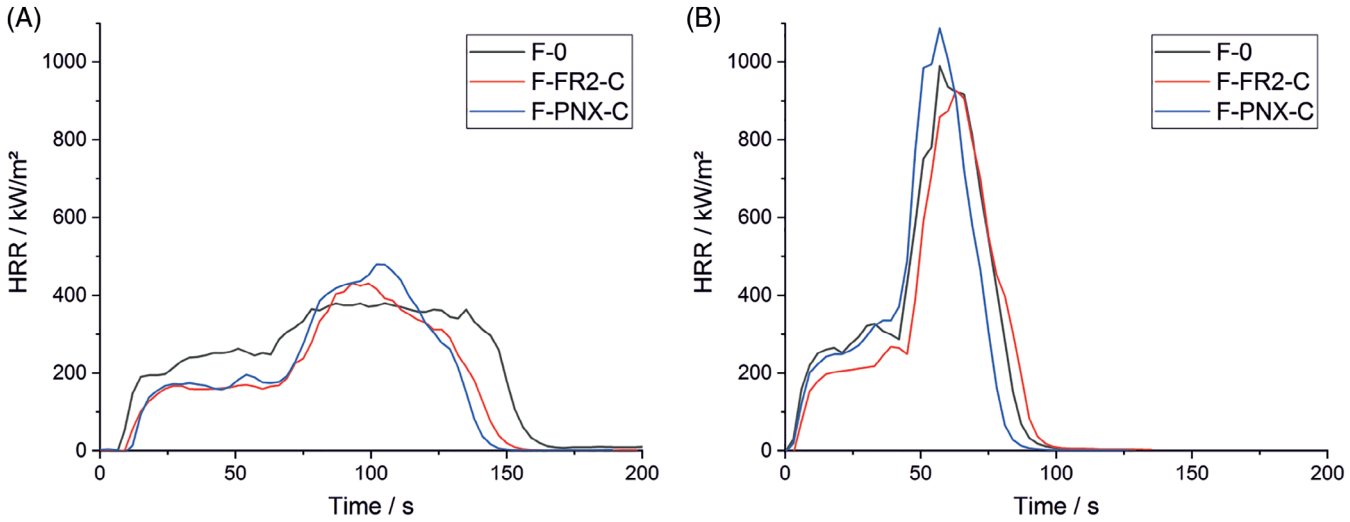

FIGURE 8 HRR curves for two tested heat fluxes: A, 20 and B, 50 kW/m^2 [Colour figure can be viewed at wileyonlinelibrary.com]

FR-2 and PNX increase the PHRR, whereby the increase due to PNX is significantly more pronounced. However, a comparison of the influence on the average heat release during the collapse stage shows substantial improvement in burning behavior. For all heat fluxes, the avHRR$_1$ of the flame-retarded foams is clearly decreased with respect to *F*-0. The decline is most distinct for the foam containing 10 php of FR-2.

The results for avHRR$_1$ correlate with the observations made in the flammability tests. However, while PNX appeared predominant with respect to its efficiency in the LOI and UL 94 test, FR-2 was more effective in reducing the heat release during the collapse stage in the cone calorimeter test. Since the FRs are effective only in the first stage of combustion, they show significance in the flammability tests. This behavior is known for FRs active in the gas phase. A significant effect can be measured in flammability tests, but the effect in a developing fire scenario might be negligibly low.[56]

The effect of the highest concentrations of FRs on the HRR is displayed in Figure 8 for heat fluxes of 20 and 50 kW/m^2. It is clearly shown that the general overall burning behavior is unchanged despite the modification of the foam formulation with FRs. Still, the burning behavior is dominated by the two steps of thermal foam decomposition, and the intensity of burning of the pool fire increases drastically with rising heat flux. Figure 8A also presents how the avHRR$_1$ is decreased for the flame-retarded foams and their PHRR is increased. The corresponding plots for heat fluxes of 25 and 35 kW/m^2 are displayed in the Supporting Information (Figure S1).

4 | CONCLUSIONS

All tested foams exhibited the typical burning behavior of cellular polymers with a short t_{ig} and rapid flame spread which is based on their morphology.[4] TG analysis of the pyrolysis behavior revealed the known two-step decomposition behavior that also dominates the burning behavior in real world fire scenarios and is due to the chemical structure of the foams.[9,37] Flammability was measured with the LOI and UL 94 HBF test. Results showed that the LOI was significantly increased for both FRs but levelled off at higher loadings. PNX was more efficient in terms of LOI increase. This was confirmed by the results of UL 94 HBF, where burning dripping was prevented by an amount of just 5 php PNX in the foam. The effect on the burning rate (ν) also levelled off at higher loadings. Since the relation between the FR concentration and the outcome of LOI and ν are non-linear, the formulations are a promising basis for multicomponent systems.

Rheological measurements of pyrolyzed material gave evidence of the reason for the improved melt flow and dripping behavior lying in the viscosity of the pyrolyzed foams. Collected drops of flame-retarded FPUFs exhibited increased viscosity. This effect was more pronounced for foams containing PNX. Also, a correlation was found between the rheological measurements and the positive results from the UL 94 HBF test. The increase in viscosity was in good agreement with the residues obtained in TG. It is therefore suggested that the increase in viscosity is caused by the condensed-phase activity of the FRs.

The two-step decomposition behavior that was measured under pyrolytic conditions also determined the fire phenomena under forced-flaming conditions in the cone calorimeter, namely structural collapse and pool fire formation. This was proven by dividing the two stages and comparing their TML and EHC. The TML of both stages was in accordance with the mass losses measured in TG, and the significantly decreased EHC and avHRR$_1$ for the collapse stage gave evidence of flame inhibition taking place during the collapse.

In the chosen test conditions, the FRs exhibited a detrimental effect on PHRR. However, the total amount of heat release significantly decreased. The FR effect was limited to the first stage of combustion, where the average rate of heat release was significantly decreased. This decrease was more pronounced for FR-2 than for PNX. The effectivity of the FRs in the first stage correlates well with the flammability test results. Protection goals of these tests are

focused mainly on the prevention of fires to develop and this is what both tested FRs do. They decrease the hazard of contributing to a fire by increased LOI, lowered burning rate, decreased FIGRA and avHRR$_1$ as well as improved dripping behavior by increasing the melt viscosity.

This paper is focused on the fire phenomena of FPUFs and investigates the burning behavior to point out possible relationship between material properties and the resulting fire phenomena. A systematic comparison of two commercially available FRs is given and it was shown that additional flame-retardant modes of action are required to further improve burning behavior. Increased condensed-phase action leading to the formation of a protective layer could decrease the PHRR and the fire load of the pool fire. This can be realized using a multicomponent system that utilizes activity in both the condensed and the gas phases.

ACKNOWLEDGMENTS

Primarily, the authors want to thank Zhihao Chen for the preparation of the foams and their characterization. Thanks go to Patrick Klack as well as Sandra Gómez-Fernández for their assistance with the cone calorimeter tests, and to Tobias Kukofka and Philip Nickl for the LOI and UL 94 HBF measurements. Further, the authors thank Aleksandra Sut for her support with the TG experiments; the help of Christian Huth with the rheological measurements was also highly appreciated.

CONFLICT OF INTEREST

The authors declare no potential conflict of interest.

ORCID

Bernhard Schartel https://orcid.org/0000-0001-5726-9754

REFERENCES

1. Engels H-W, Pirkl H-G, Albers R, et al. Polyurethanes: versatile materials and sustainable problem solvers for Today's challenges. *Angew Chem Int Ed*. 2013;52(36):9422-9441.
2. Szycher M. Rigid Polyurethane Foams. *Szycher's Handbook of Polyurethanes*. 2nd ed.Boca Raton, FL: CRC Press; 2012:257-308.
3. Hilado CJ. Flammability characteristics of cellular plastics. *Industrial & Engineering Chemistry Product Research and Development*. 1967;6 (3): 154–166. http://dx.doi.org/10.1021/i360023a004.
4. Drysdale DD. Fundamentals of the fire behaviour of cellular polymers. In: Buist JM, Grayson SJ, Woolley WD, eds. *Fire and Cellular Polymers*. Dordrecht: Springer Netherlands; 1986:61-75.
5. Hirschler MM. Polyurethane foam and fire safety. *Polym Adv Technol*. 2008;19(6):521-529.
6. Lounis M, Leconte S, Rousselle C, et al. Fireproofing of domestic upholstered furniture: migration of flame retardants and potential risks. *J Hazard Mater*. 2019;366:556-562.
7. Günther M, Lorenzetti A, Schartel B. Fire phenomena of rigid polyurethane foams. *Polymers*. 2018;10(10):1166.
8. Günther M, Lorenzetti A, Schartel B. From cells to residues: flame-retarded rigid polyurethane foams. *Combust Sci Technol*. 2019;1-29.
9. Krämer RH, Zammarano M, Linteris GT, Gedde UW, Gilman JW. Heat release and structural collapse of flexible polyurethane foam. *Polym Degrad Stab*. 2010;95(6):1115-1122.
10. Zammarano M, Krämer RH, Harris R, et al. Flammability reduction of flexible polyurethane foams via carbon nanofiber network formation. *Polym Adv Technol*. 2008;19(6):588-595.
11. Stone H, Pcolinsky JM, Parrish DB, Beal GE. The effect of foam density on combustion characteristics of flexible polyurethane foam. *J Cell Plast*. 1991;27(1):78-79.
12. Wang Y, Kang W, Chen C, et al. Combustion behaviour and dominant shrinkage mechanism of flexible polyurethane foam in the cone calorimeter test. *J Hazard Mater*. 2019;365:395-404.
13. Lefebvre J, Bastin B, Le Bras M, et al. Flame spread of flexible polyurethane foam: comprehensive study. *Polym Test*. 2004;23(3): 281-290.
14. Lefebvre J, Bastin B, Le Bras M, Duquesne S, Paleja R, Delobel R. Thermal stability and fire properties of conventional flexible polyurethane foam formulations. *Polym Degrad Stab*. 2005;88(1):28-34.
15. Kashiwagi T. Polymer combustion and flammability—role of the condensed phase. *Symp (Int) Combust*. 1994;25(1):1423-1437.
16. Stoliarov SI, Zeller O, Morgan AB, Levchik S. An experimental setup for observation of smoldering-to-flaming transition on flexible foam/fabric assemblies. *Fire Mater*. 2018;42(1):128-133.
17. Hadden R, Alkatib A, Rein G, Torero JL. Radiant ignition of polyurethane foam: the effect of sample size. *Fire Technol*. 2014;50(3):673-691.
18. Gómez-Fernández S, Günther M, Schartel B, Corcuera MA, Eceiza A. Impact of the combined use of layered double hydroxides, lignin and phosphorous polyol on the fire behavior of flexible polyurethane foams. *Ind Crops Prod*. 2018;125:346-359.
19. Rao W-H, Xu H-X, Xu Y-J, et al. Persistently flame-retardant flexible polyurethane foams by a novel phosphorus-containing polyol. *Chem Eng J*. 2018;343:198-206.
20. Przystas A, Jovic M, Salmeia KA, et al. Some key factors influencing the flame Retardancy of EDA-DOPO containing flexible polyurethane foams. *Polymers*. 2018;10(10):1115.
21. Wang X, Zhang P, Huang Z, Xing W, Song L, Hu Y. Effect of aluminum diethylphosphinate on the thermal stability and flame retardancy of flexible polyurethane foams. *Fire Saf J*. 2019;106:72-79.
22. Levchik SV, Weil ED. New developments in flame retardancy of styrene thermoplastics and foams. *Polym Int*. 2008;57(3):431-448.
23. Wang JQ, Chow WK. A brief review on fire retardants for polymeric foams. *J Appl Polym Sci*. 2005;97(1):366-376.
24. Singh H, Jain AK. Ignition, combustion, toxicity, and fire retardancy of polyurethane foams: a comprehensive review. *J Appl Polym Sci*. 2009; 111(2):1115-1143.
25. Rao W-H, Liao W, Wang H, Zhao H-B, Wang Y-Z. Flame-retardant and smoke-suppressant flexible polyurethane foams based on reactive phosphorus-containing polyol and expandable graphite. *J Hazard Mater*. 2018;360:651-660.
26. Weil ED, Levchik SV. Flame Retardants in Commercial Use or Advanced Development in Polyurethanes. *Flame Retardants for Plastics and Textiles*. Carl Hanser Verlag GmbH & Co. KG; 2009: 153-178.
27. Velencoso MM, Battig A, Markwart JC, Schartel B, Wurm FR. Molecular firefighting—how modern phosphorus chemistry can help solve the challenge of flame Retardancy. *Angew Chem Int Ed*. 2018;57(33): 10450–10467.
28. Vanspeybroeck R, Van Hees P, Vandevelde P. Combustion behaviour of polyurethane flexible foams under cone Calorimetry test conditions. *Fire Mater*. 1993;17(4):155-166.
29. Xiao-Yu C, Zong-Hou H, Xiu-Qi X, Jia L, Xin-Yu F, Zhan W. Synergistic effect of carbon and phosphorus flame retardants in rigid polyurethane foams. *Fire Mater*. 2018;42(4):447-453.
30. Schartel B, Bartholmai M, Knoll U. Some comments on the use of cone calorimeter data. *Polym Degrad Stab*. 2005;88(3):540-547.
31. Schartel B, Wilkie CA, Camino G. Recommendations on the scientific approach to polymer flame retardancy: part 1—scientific terms and methods. *J Fire Sci*. 2016;34(6):447-467.
32. Clearly TG, Quintiere J. *Flammability Characterization of Foam Plastics*. NISTIR4664. Gaithersburg: NIST; 1991.

33. Schartel B, Hull TR. Development of fire-retardedmaterials—interpretation of cone calorimeter data. *Fire Mater*. 2007;31(5):327-354.
34. Pau DSW, Fleischmann CM, Delichatsios MA. Apparatus for investigating the burning and dripping of vertically oriented polyurethane foams. *Fire Mater*. 44(2):211-229.
35. Galaska ML, Morgan AB, Schenck KA, Stalter JG. Apparatus for the vertical orientation cone calorimeter testing of flexible polyurethane foams. *Fire Mater*. 2016;40(1):158-176.
36. Mills NJ. The wet kelvin model for air flow through open-cell polyurethane foams. *J Mater Sci*. 2005;40(22):5845-5851.
37. Prasad KR, Krämer R, Marsh ND, Nyden MR, Ohlemiller TJ, Pitts WM, Zammarano M. Numerical Simulation of fire spread on polyurethane foam slabs. *Proceedings of the Fire and Materials Conference*, San Francisco; 2009.
38. Rogers FE, Ohlemiller TJ. Pyrolysis kinetics of a polyurethane foam by Thermogravimetry; a general kinetic method. *J Macromol Sci Part A Chem*. 1981;15(1):169-185.
39. Sut A, Metzsch-Zilligen E, Großhauser M, Pfaendner R, Schartel B. Rapid mass calorimeter as a high-throughput screening method for the development of flame-retarded TPU. *Polym Degrad Stab*. 2018;156:43-58.
40. Sut A, Metzsch-Zilligen E, Großhauser M, Pfaendner R, Schartel B. Synergy between melamine cyanurate, melamine polyphosphate and aluminum diethylphosphinate in flame retarded thermoplastic polyurethane. *Polym Test*. 2019;74:196-204.
41. Ravey M, Keidar I, Weil ED, Pearce EM. Flexible polyurethane foam. II. Fire retardation by tris(1,3-dichloro-2-propyl) phosphate part a. examination of the vapor phase (the flame). *J Appl Polym Sci*. 1998;68(2):217-229.
42. Perret B, Pawlowski KH, Schartel B. Fire retardancy mechanisms of arylphosphates in polycarbonate (PC) and PC/acrylonitrile-butadiene-styrene. *J Therm Anal Calorim*. 2009;97(3):949-958.
43. Ravey M, Pearce EM. Flexible polyurethane foam .1. Thermal decomposition of a polyether-based, water-blown commercial type of flexible polyurethane foam. *J Appl Polym Sci*. 1997;63(1):47-74.
44. Woolley WD. Nitrogen-containing products from the thermal decomposition of flexible polyurethane foams. *Br Polym J*. 1972;4(1):27-43.
45. van Krevelen DW. Some basic aspects of flame resistance of polymeric materials. *Polymer*. 1975;16(8):615-620.
46. Liang S, Neisius M, Mispreuve H, Naescher R, Gaan S. Flame retardancy and thermal decomposition of flexible polyurethane foams: structural influence of organophosphorus compounds. *Polym Degrad Stab*. 2012;97(11):2428-2440.
47. Brehme S, Köppl T, Schartel B, Altstädt V. Competition in aluminium phosphinate-basedhalogen-free flame retardancy of poly(butylene terephthalate) and its glass-fibre composites. *e-Polym*. 2014;14(3):193-208.
48. Lin B, Yuen ACY, Li A, et al. MXene/chitosan nanocoating for flexible polyurethane foam towards remarkable fire hazards reductions. *J Hazard Mater*. 2020;381:120952.
49. Langfeld K, Wilke A, Sut A, et al. Halogen-free fire retardant styrene-ethylene-butylene-styrene-based thermoplastic elastomers using synergistic aluminum diethylphosphinate-based combinations. *J Fire Sci*. 2015;33(2):157-177.
50. Schartel B, Wilkie CA, Camino G. Recommendations on the scientific approach to polymer flame retardancy: part 2—concepts. *J Fire Sci*. 2016;35(1):3-20.
51. Matzen M, Kandola B, Huth C, Schartel B. Influence of flame retardants on the melt dripping behaviour of thermoplastic polymers. *Materials*. 2015;8(9):5621-5646.
52. Franklin AG, Krizek RJ. Complex viscosity of a kaolin clay. *Clays Clay Miner*. 1969;17(2):101-110.
53. Diniz A, Huth C, Schartel B. Dripping and decomposition under fire: melamine cyanurate vs. glass fibres in polyamide 6. *Polym Degrad Stab*. 2019;171:109048.
54. Troitzsch JH. How do foams perform under fire conditions? In: Buist JM, Grayson SJ, Woolley WD, eds. *Fire and Cellular Polymers*. Vol 77–91. Dordrecht: Springer Netherlands; 1986.
55. Bustamante Valencia, L, *Experimental and Numerical Investigation of the Thermal Decomposition of Materials at Three Scales: Application to Polyether Polyurethane Foam Used in Upholstered Furniture*. PhD thesis, Poitiers, France: ENSMA; 2009.
56. Gallo E, Braun U, Schartel B, Russo P, Acierno D. Halogen-free flame retarded poly(butylene terephthalate) (PBT) using metal oxides/PBT nanocomposites in combination with aluminium phosphinate. *Polym Degrad Stab*. 2009;94(8):1245-1253.
57. Levchik SV, Weil ED. Thermal decomposition, combustion and fire-retardancy of polyurethanes—a review of the recent literature. *Polym Int*. 2004;53(11):1585-1610.
58. Jayakody C, Myers D, Sorathia U, Nelson GL. Fire-retardant characteristics of water-blown molded flexible polyurethane foam materials. *J Fire Sci*. 2000;18(6):430-455.
59. Ravey M, Weil ED, Keidar I, Pearce EM. Flexible polyurethane foam. II. Fire retardation by tris(1,3-dichloro-2-propyl) phosphate. Part B. examination of the condensed phase (the pyrolysis zone). *J Appl Polym Sci*. 1998;68(2):231-254.
60. Weil ED, Levchik SV, Ravey M, Zhu W. A survey of recent Progress in phosphorus-based flame retardants and some mode of action studies. *Phosphorus Sulfur Silicon Relat Elem*. 1999;144(1):17-20.
61. Battig A, Markwart JC, Wurm FR, Schartel B. Hyperbranched phosphorus flame retardants: multifunctional additives for epoxy resins. *Polym Chem*. 2019;10(31):4346-4358.
62. Harper CA. *Handbook of Building Materials for Fire Protection*. McGraw-Hill Education; 2003.
63. Morgan, AB, Cone Calorimeter and Pyrolysis Combustion Flow Calorimeter Testing of Polyurethane Foams—A Call for Collaboration to Establish a Predictive Model. 23rd Annual Conference on Recent Advances in Flame Retardancy of Polymeric Materials, 2012, Stamford, USA.

SUPPORTING INFORMATION

Additional supporting information may be found online in the Supporting Information section at the end of this article.

How to cite this article: Günther M, Levchik SV, Schartel B. Bubbles and collapses: Fire phenomena of flame-retarded flexible polyurethane foams. *Polym Adv Technol*. 2020;31:2185–2198. https://doi.org/10.1002/pat.4939